Chinese Chemical Letters 32 (2021) 729–734

Contents lists available at ScienceDirect

Chinese Chemical Letters

journal homepage: www.elsevier.com/locate/cclet

Communication

Molecular-scale drug delivery systems loaded with oxaliplatin for supramolecular chemotherapy

Jie Yang, Dihua Dai, Lianjun Ma*, Ying-Wei Yang*

International Joint Research Laboratory of Nano-Micro Architecture Chemistry, College of Chemistry, and Department of Endoscopics, China-Japan Union Hospital of Jilin University, Jilin University, Changchun 130012, China

ARTICLE INFO

Article history:
Received 25 July 2020
Received in revised form 11 August 2020
Accepted 18 August 2020
Available online 22 August 2020

Keywords:
Drug delivery system
Host-guest chemistry
Macrocyclic chemistry
Supramolecular chemotherapy
Supramolecular chemistry

ABSTRACT

Smart strategies that can decrease the side effect and enhance the therapeutic efficacy of chemotherapy are in urgent need to meet the special demands of cancer therapy. Herein, two water-soluble macrocyclic hosts, *i.e.*, a carboxylated leaning tower[6]arene (CLT6) and a carboxylated [2]biphenyl-extended pillar[6]arene (CBpP6), are used to load chemotherapy drug oxaliplatin (OxPt) by forming inclusion complexes (OxPt⊂CLT6 and OxPt⊂CBpP6) through host-guest interactions. Interestingly, OxPt can be released from the macrocyclic cavities of these drug delivery systems (DDSs) *via* the competitive binding effect of spermine (SPM) because of the stronger binding abilities of CLT6/CBpP6 toward SPM as compared with OxPt, leading to enhanced cytotoxicity on SPM-overexpressed cancer cells, such as breast cancer MCF-7 cells. Moreover, compared to free OxPt, due to the low concentration of SPM in normal cells, OxPt⊂CLT6 and OxPt⊂CBpP6 demonstrated a decreased cytotoxicity on liver L02 cells, which is beneficial for reducing the side effect of anticancer drug during chemotherapy. Such a strategy might be extended to other antitumor drugs and water-soluble macrocycles with suitable cavity sizes to achieve controllable drug delivery and enhanced anticancer ability in supramolecular chemotherapy.

As a widely used method for cancer treatment, chemotherapy still suffers from some intrinsic disadvantages such as low selectivity, tumour resistance and undesired side effects, which seriously weaken the therapeutic effect [1–3]. Considering the miserable shortcomings of chemotherapy, the development of effective drug delivery systems (DDSs) to improve the therapeutic effect and realize the controlled release of anticancer drugs is of great significance [4–7]. In the last few decades, various DDSs, including inorganic nanomaterials, organic nanocarriers, and organic-inorganic nanohybrids have been designed and extensively fabricated [8–13]. Notably, the synthesis and decoration of inorganic nanomaterials are not difficult, but their biodistribution, biodegradation, metabolic mechanisms and immunogenicity need to be comprehensively studied and clearly understood [14–16]. On the other hand, organic carriers with the engaging features of biodegradability and biocompatibility are capable of carrying drugs *via* physical encapsulation or covalent bonding, but will cause unpredictable drug loading and premature drug leakage [17–19]. Thus, the emergence of organic nanocarriers with predictable drug loading capacity can satisfy the demands of controllable drug delivery as well as enrich the toolbox of DDSs [20,21].

As a kind of host molecules that can selectively accommodate molecules or ionic guests *via* host-guest interactions, supramolecular macrocycles have been widely used to construct dynamic multifunctional materials [22–26]. Taking advantages of the noncovalent interactions between various hosts and guests, supramolecular macrocycles bearing highly tuneable combinations and intelligent stimuli-responsive properties are widely developed for gas capture and separation [27,28], sensing and detection [29–33], supramolecular self-assembly [34–36] and controlled drug delivery [37–42]. Particularly, as a new group of synthetic macrocycles, pillar[*n*]arenes (n = 5–15) [43–47], especially pillar[5,6]arenes and their derivatives, have been widely used in biomedicine due to their appropriate cavity sizes and good biocompatibility [48–53]. Based on the original features of pillar[6]arene, it leads to further breakthroughs to extend the application of supramolecular chemistry, however, there are still some deficiencies that need to be optimized in terms of synthesis yield, cavity backbone adaptability and variability of substituent numbers [54]. In order to tackle this problem, in 2016–2018, our group successfully designed and reported two novel macrocyclic arenes, namely a [2]biphenyl-extended pillar[6]arene (BpP6) and a leaning tower[6]arene (LT6), with high synthetic yield, good cavity

* Corresponding authors.
E-mail addresses: horsejlm@jlu.edu.cn (L. Ma), ywyang@jlu.edu.cn (Y.-W. Yang).

https://doi.org/10.1016/j.cclet.2020.08.035
1001-8417/

adaptability, less substituents and prominent guest binding capability [55,56]. The rigid backbone and large cavity endow BpP6 with prominent properties, such as the purification of petrochemicals and detection of hazardous substances. Meanwhile, water-soluble cationic BpP6 and LT6 possessed good recognition capabilities for sulfonate guests in aqueous solutions. On the other hand, owing to the adaptability of cavity adaptability and variability of substituent numbers, both LT6 and BpP6 possess enhanced guest binding capabilities [56,57]. On the basis of the abovementioned studies and the unique properties of water-soluble supramolecular macrocycle derivatives [58–60], we envision that utilizing ionic LT6/BpP6 to construct novel DDSs would be an efficient strategy for anticancer drug delivery.

Herein, we firstly designed and synthesized two macrocyclic receptors as molecular-scale biocompatible drug carriers, namely carboxylated leaning tower[6]arene (CLT6) and carboxylated [2] biphenyl-extended pillar[6]arene (CBpP6), for the *in vitro* delivery of anticancer drug oxaliplatin (OxPt) (Fig. 1). Through the host-guest interactions, OxPt guest was spontaneously encapsulated in the cavities of CLT6 or CBpP6 host to construct host-guest complex of OxPt⊂CLT6 or OxPt⊂CBpP6 with a stoichiometry of 1:1. The association constants were calculated as $(1.15 \pm 0.08) \times 10^3$ L/mol and $(2.29 \pm 0.19) \times 10^2$ L/mol, respectively. In addition, spermine (SPM), overexpressed in MCF-7 cancer cells, could also be encapsulated into CLT6 and CBpP6 cavities to develop 1:1 SPM⊂CLT6 or SPM⊂CBpP6 complex. Moreover, because of the stronger binding abilities between both two macrocycles and SPM with a binding constant of $(4.59 \pm 0.82) \times 10^4$ L/mol for SPM⊂CLT6 and $(2.64 \pm 0.61) \times 10^4$ L/mol for SPM⊂CBpP6, respectively, OxPt could be released from OxPt⊂CLT6 or OxPt⊂CBpP6 complex, and SPM was simultaneously bound in the corresponding cavities of hosts, causing enhanced cytotoxicity on MCF-7 cells. Interestingly, compared with free OxPt, such two complexes also exhibited a reduced toxicity on L02 cells, which was attributed to the low SPM content in normal L02 cells.

The synthetic routes to CLT6 and CBpP6 were shown in Fig. S1 (Supporting information). According to our previous report, CLT6 and CbBpP6 were synthesized by demethylation, etherification and hydrolysis of LT6 [32,56]. Subsequently, after a facile neutralization, CLT6/CBpP6 host with eight carboxylate groups were obtained in satisfactory yields, which have been characterized by ^{1}H NMR, ^{13}C NMR and MALDI-TOF-MS spectroscopy (Figs. S2–S6 in Supporting information).

To investigate the host-guest interactions between the two macrocycles and OxPt, ^{1}H NMR experiments were performed. As shown in Fig. 2A, upon addition of 1.0 equiv. of CLT6, all the proton signals (H_a, H_b, H_c, H_d and H_e) of OxPt showed considerable upfield shifts ($\Delta\delta$ = −1.31, −1.40, −1.27, −1.05 and −1.24 ppm, respectively),

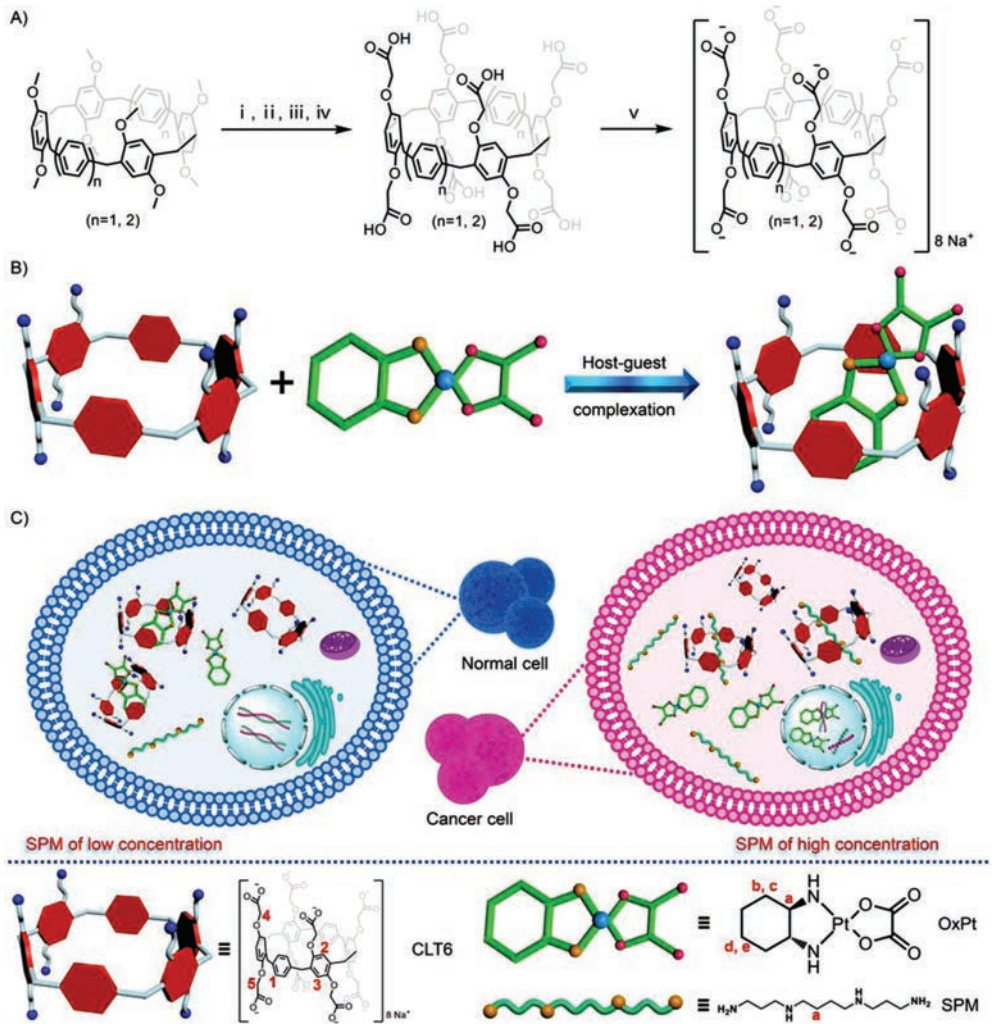

Fig. 1. Schematic illustration of the preparation of CLT6/CBpP6 (n = 1, 2, respectively) DDS and its application for *in vitro* OxPt delivery. (A) Synthetic route to CLT6. (i) BBr_3, DCM, room temperature; (ii) $BrCH_2COOEt$, NaH, THF, reflux; (iii) NaOH, H_2O, THF, reflux; (iv) HCl; (v) NaOH, H_2O. (B, C) OxPt⊂CLT6 was prepared *via* host-guest complexation of CLT6 host and anticancer drug OxPt, showing a reduced toxicity on normal cells and an enhanced cytotoxic effect on cancer cells.

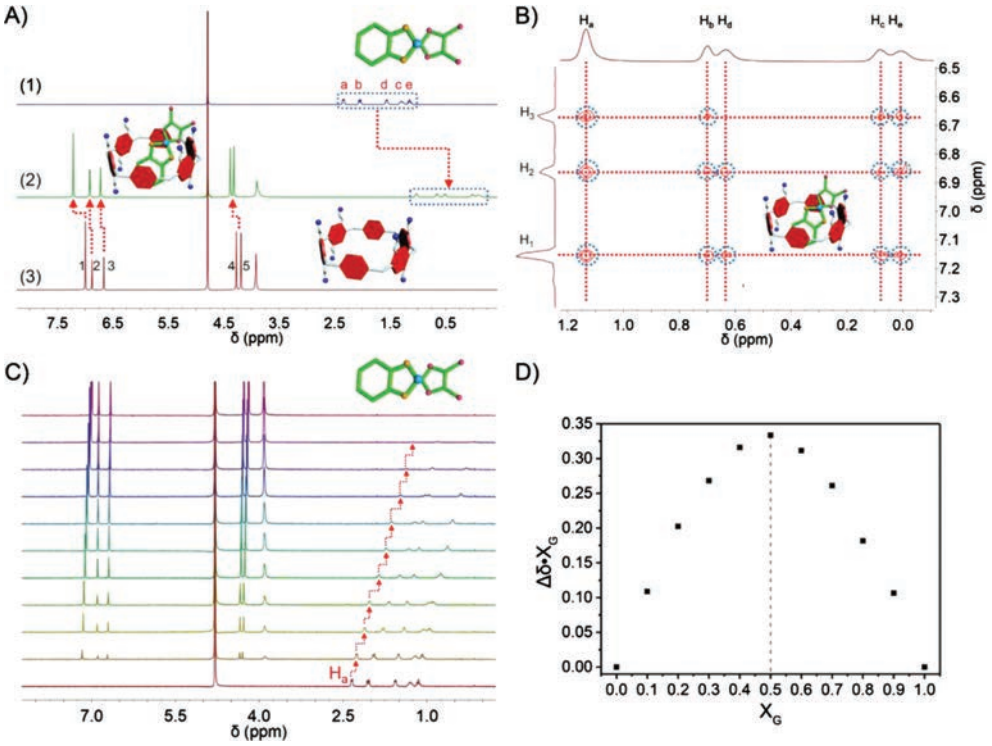

Fig. 2. (A) ^{1}H NMR spectra (400 MHz, 298 K): (1) OxPt (5.00 mmol/L) in D_2O; (2) mixture solution of OxPt and CLT6 (5.00 mmol/L); (3) CLT6 (5.00 mmol/L) in D_2O. (B) Partial 2D ROESY spectrum (600 MHz, 298 K) of CLT6 (5 mmol/L) with OxPt (5 mmol/L) in D_2O with a mixing time of 300 ms. (C) ^{1}H NMR spectra of different radios of CLT6 and OxPt (from top to bottom: CLT6:OxPt = 10:0, 9:1, 8:2, 7:3, 6:4, 5:5; 4:6, 3:7, 2:8 1:9 and 0:10). (D) Job's plot analysis of CLT6 and OxPt.

reflecting the shielding effect of macrocyclic cavity on OxPt. Meanwhile, the downfield shifts of proton signals (H_1, H_2, H_3, H_4 and H_5) in CLT6 were attributed to the deshielding effect caused by OxPt. Besides, the similar changes ($\Delta\delta$ = −0.53, −0.59, −0.58, −0.58 and −0.57 ppm for H_a, H_b, H_c, H_d and H_e of OxPt, respectively) were also observed in the OxPt⊂CBpP6 complex (Fig. S7 in Supporting information). Subsequently, the host-guest interactions between CLT6/CBpP6 and OxPt were further investigated by 2D ROESY spectroscopy. Clear correlations between phenylene protons (H_1, H_2 and H_3) in CLT6 or phenylbenzene protons (H_1, H_2, H_3 and H_4) in CBpP6 and cyclohexyl protons (H_a, H_b, H_c, H_d and H_e) in OxPt were displayed, indicating the inclusion complexation between CLT6/CBpP6 and OxPt (Fig. 2B and Fig. S8 in Supporting information). Furthermore, in order to verify the formation of host-guest complex, the 2D diffusion-ordered NMR spectroscopy (DOSY) experiments were conducted. The results showed that the weight-average diffusion coeffcients (D) of OxPt⊂CLT6 and OxPt⊂CBpP6 were determined to be 3.94×10^{-10} m^2/s and 1.81×10^{-11} m^2/s, respectively, which were lower than that of OxPt (4.77×10^{-10} m^2/s), illustrating the formation of host-guest complex (Figs. S9 and S10 in Supporting information). All the above experiments proved the formation of the host-guest complexes (OxPt⊂CLT6, OxPt⊂CBpP6) between the anticancer drug OxPt and CLT6 (or CBpP6) with an electron-rich cavity.

To further study the binding mode of macrocycle hosts and OxPt guest, Job's plot analysis was conducted. ^{1}H NMR spectra of the mixture of CLT6 (or CBpP6) and OxPt with various molar ratios from 0:10 to 10:0 were recorded. According to the Job's plot analysis for proton shift (H_a) of OxPt in various mixtures, the molar fraction of OxPt is 0.5 at the maximum, indicating the 1:1 binding stoichiometry between CLT6/CBpP6 and OxPt (Figs. 2C and D, Fig. S11 in Supporting information). Meanwhile, ^{1}H NMR titration demonstrated that the association constants (K_a) of CLT6 (or CBpP6) and OxPt were $(1.15 \pm 0.08) \times 10^3$ L/mol and $(2.29 \pm 0.19) \times 10^2$ L/mol for OxPt⊂CLT6 and OxPt⊂CBpP6, respectively (Figs. S12 and S13 in Supporting information). The biphenyl units in CBpP6 skeleton expanded the cavity size of CBpP6 and weakened the host-guest interaction between CBpP6 and OxPt, resulting in a smaller K_a for OxPt⊂CBpP6 [55].

Controlled release of the anticancer drug at the tumour site can improve the therapeutic effect and reduce drug side effects [61–63]. Therefore, SPM, an overexpressed endogenous polyamine molecule in most tumour cells that promotes cell proliferation [64,65], was selected as a stimulus to activate the controllable release of OxPt or other suitable drugs from the DDSs [66–70]. As shown in Figs. 3A–C and Figs. S14 and S15 (Supporting information), Job's plot analysis demonstrated the existence of host-guest interaction and 1:1 binding mode of CLT6/CBpP6 and SPM through host-guest interactions, suggesting the formation of SPM⊂CLT6 (or SPM⊂CBpP6). The stronger binding affinities of two DDSs with SPM were conducive to the release of OxPt from the formed host-guest complex [71]. Thus, ^{1}H NMR titration experiments were carried out to measure the K_a between two hosts and SPM. As in Fig. S16 (Supporting information), the K_a was determined to be $(4.59 \pm 0.82) \times 10^4$ L/mol and $(2.64 \pm 0.61) \times 10^4$ L/mol for SPM⊂CLT6 and SPM⊂CBpP6, respectively. Compared with the K_a values of OxPt⊂CLT6 ($(1.15 \pm 0.08) \times 10^3$ L/mol) and OxPt⊂CBpP6 ($(2.29 \pm 0.19) \times 10^2$ L/mol), the higher K_a values of SPM⊂CLT6 and SPM⊂CBpP6 were about 40 times and 115 times of that of OxPt⊂CLT6 and OxPt⊂CBpP6, respectively. This fact effectively promotes the competitive binding-triggered release of OxPt in the DDSs and the consumption of intracellular SPM, suggesting the great potential of our design in anticancer application.

Subsequently, to study the effectively competitive effect of SPM molecules to OxPt, UV–vis spectra were employed to monitor the drug release of OxPt from the DDSs complexes. With the increase of SPM, the absorbance of OxPt⊂CLT6 or OxPt⊂CBpP6 gradually decreased, revealing that OxPt was released from the DDSs (Fig. 3D and Fig. S17 in

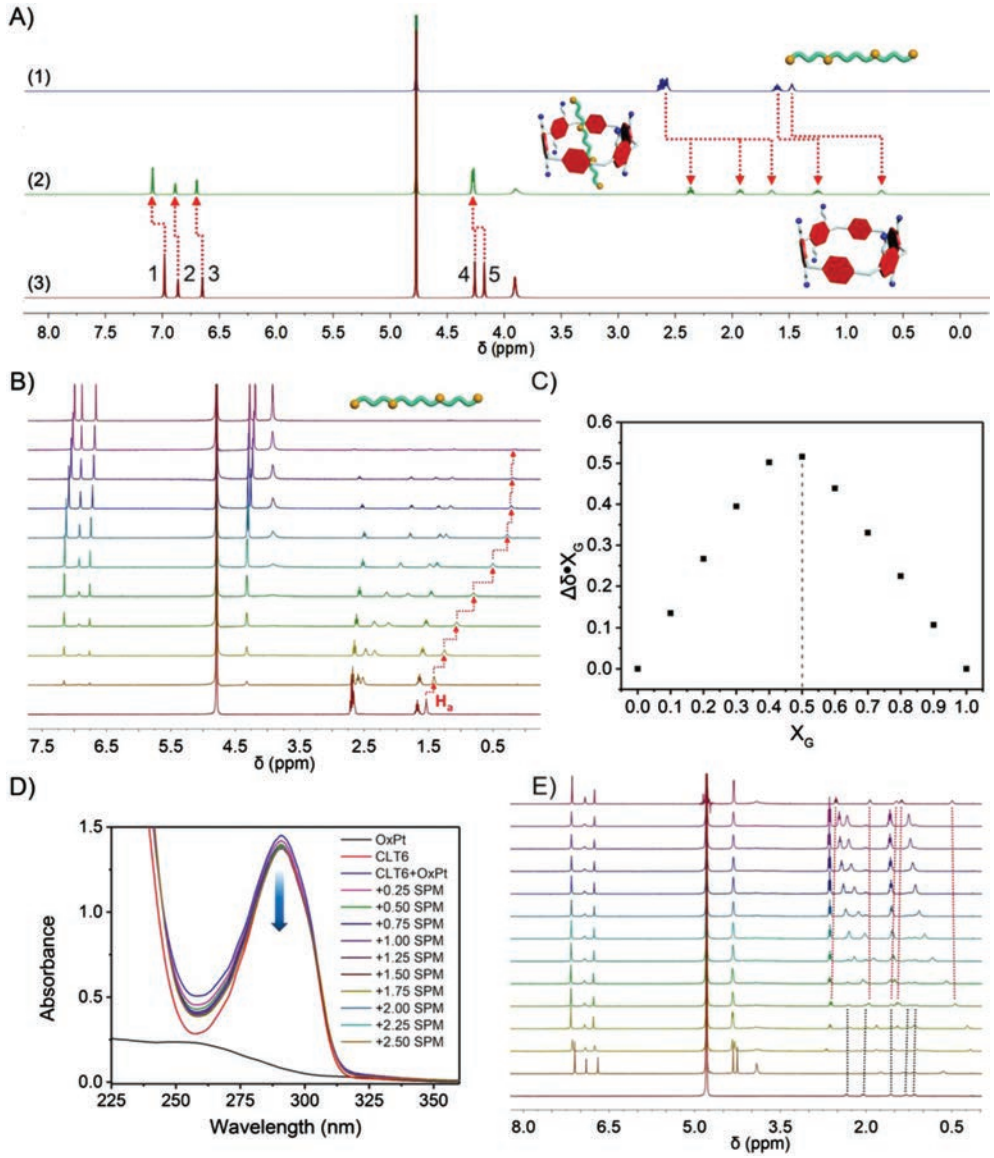

Fig. 3. (A) ^{1}H NMR spectra (400 MHz, 298 K): (1) SPM (5.00 mmol/L) in D_2O; (2) mixed solution of SPM and CLT6 (5.00 mmol/L); (3) CLT6 (5.00 mmol/L) in D_2O. (B) ^{1}H NMR spectra of different ratios of CLT6 and SPM (from top to bottom: CLT6:SPM = 10:0, 9:1, 8:2, 7:3, 6:4, 5:5; 4:6, 3:7, 2:8 1:9 and 0:10). (C) Job's plot analysis of CLT6 and SPM binding. (D) UV–vis spectra of OxPt (100 μmol/L), CLT6 (100 μmol/L) and CLT6 + OxPt (100 μmol/L) with different amounts (0-2.5 equiv.) of SPM. (E) ^{1}H NMR spectra (400 MHz, 298 K) of (from bottom to top) OxPt (0.5 mmol/L), CLT6 + OxPt (0.5 mmol/L) with various amounts (0.2, 0.4, 0.5, 0.6, 0.8, 1.0, 1.2, 1.4, 1.6, 1.8, 2.0 equiv.) of SPM, and CLT6 + SPM (0.5 mmol/L).

Supporting information). Subsequently, ^{1}H NMR titration studies were established to visually observe the competitive effect of SPM and the release of OxPt. As the concentration of SPM increased, the proton signals of OxPt in OxPt⊂CLT6 or OxPt⊂CBpP6 shifted back to downfield, indicating the host-guest complexes of OxPt⊂CLT6 and OxPt⊂CBpP6 were destroyed generally. Notably, when the equivalent ratio of SPM to free OxPt was 1:1, the chemical shifts of OxPt proton in the host-guest complex was consistent with that in free OxPt, which illustrated the release of OxPt from OxPt⊂CLT6 or OxPt⊂CBpP6 (Fig. 3E and Fig. S18 in Supporting information). Meanwhile, the proton signals of SPM showed upfield shifts, further confirming that SPM occupied the cavities of CLT6 and CBpP6. All the experimental results indicated that SPM could effectively bind with CLT6 and CBpP6 in a competitive manner, leading to the release of OxPt from OxPt⊂CLT6 and OxPt⊂CBpP6 on command for cancer therapy.

The biocompatibility of CLT6 and CBpP6 was evaluated *via* cytotoxicity study on L02 cells and MCF-7 cells, and hemolysis test on red blood cells (RBCs). As shown in Fig. 4A and Fig. S19A (Supporting information), 3-(4′,5′-dimethylthiazol-2′-yl)-2,5-diphenyl tetrazolium bromide (MTT) assay results showed high cells viability (>90%) after the cells incubated with CLT6/CBpP6 host at a concentration range of 0−100 μmol/L for 24 h, indicating good biocompatibility of CLT6. Moreover, the hemolysis rates of CLT6 and CBpP6 were well <10% even at a high concentration of 500 μmol/L, suggesting its negligible destructiveness on RBCs (Fig. 4B and Fig. S19B in Supporting information).

As aforementioned, SPM could effectively compete with OxPt from the cavities of the macrocycles to achieve the goal of drug release and SPM consumption according to the UV–vis and ^{1}H NMR spectra studies. To further investigate the side effect of the systems on normal cells and the antitumor effect on tumour cells caused by SPM regulating OxPt⊂CLT6/OxPt⊂CBpP6, L02 cells (normal cells with low SPM concentration) and MCF-7 cells (tumour cells with high SPM concentration) were selected as the model cells to conduct MTT assay *in vitro*. After incubation with free OxPt, OxPt⊂CLT6 or OxPt⊂CBpP6 for 24 h, as the concentration of free

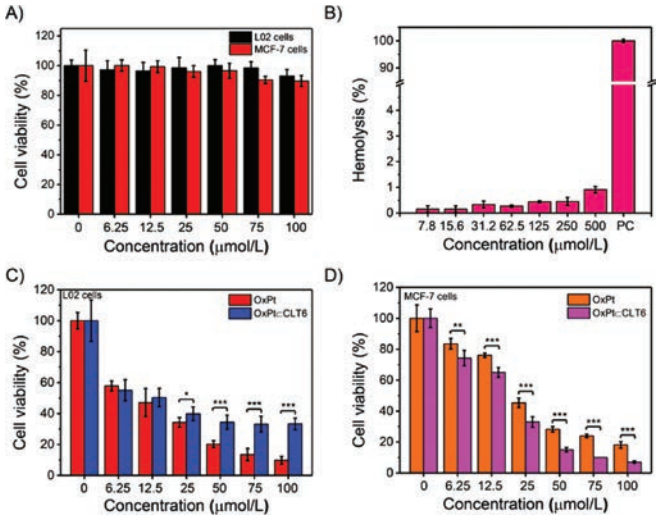

Fig. 4. (A) Cell viabilities of L02 cells and MCF-7 cells treated by CLT6 host for 24 h. (B) Hemolysis test of CLT6 (PC represents positive control group). Cell viabilities of (C) L02 cells and (D) MCF-7 cells incubated with free OxPt and OxPt⊂CLT6 for 24 h (*$P <$ 0.05, **$P <$ 0.01, ***$P <$ 0.001).

OxPt, OxPt⊂CLT6 or OxPt⊂CBpP6 increased, cell viabilities of L02 and MCF-7 cells gradually decreased. Importantly, compared with free OxPt, both OxPt⊂CLT6 and OxPt⊂CBpP6 exhibited lower cytotoxicity at the same concentration, which was attributed to the weak competitive effect of low SPM concentration in normal cells on OxPt in the OxPt⊂CLT6/OxPt⊂CBpP6 system (Fig. 4C and Fig. S20 in Supporting information). Moreover, due to the size-fit effect for the suitable cavity of CLT6 and the molecular size of OxPt, OxPt⊂CLT6 showed a reduced toxicity to L02 cells than that of OxPt⊂CBpP6. Interestingly, cell viabilities results indicated that both OxPt⊂CLT6 and OxPt⊂CBpP6 complexes possessed improved cytotoxicity on MCF-7 cells compared to free OxPt (Fig. 4D and Fig. S21 in Supporting information), revealing the effective competitive effect of SPM to OxPt. In addition, because of the higher association constant between CLT6 and OxPt, OxPt⊂CLT6 demonstrated enhanced cytotoxicity on MCF-7 cells than that of OxPt⊂CBpP6, which was consistent with the aforementioned binding studies. All the experimental results indicated that both OxPt⊂CLT6 and OxPt⊂CBpP6 showed decreased side effect to L02 cells and improved cytotoxicity on MCF-7 cells.

In summary, two water-soluble macrocyclic receptors, namely CLT6 and CBpP6, were designed as molecular-scale biocompatible drug carriers to build DDSs OxPt⊂CLT6 or OxPt⊂CBpP6 with the marriage of anticancer drug OxPt *via* host-guest interaction for enhanced anticancer ability and reduced side effect in chemotherapy. OxPt could be spontaneously encapsulated in the cavity of CLT6/CBpP6 host to generate OxPt⊂CLT6 or OxPt⊂CBpP6 complex with a stoichiometry of 1:1, respectively. Compared with free OxPt, CLT6/CBpP6 possess higher binding ability with SPM, OxPt could be released from the two host-guest complexes through competitive substitution effect of SPM, gaining enhanced cytotoxicity on SPM overexpressed breast cancer MCF-7 cells. Interestingly, the decreased side effect was obtained on L02 cells due to the effective binding effect of the CLT6/CBpP6 host toward OxPt and the low SPM levels in L02 cells. This strategy might be extended to other antitumor drugs and water-soluble synthetic macrocycles with appropriate cavity sizes to realize controllable drug release and enhanced anticancer ability.

Declaration of competing interest

The authors report no declarations of interest.

Acknowledgments

We acknowledge the National Natural Science Foundation of China (No. 21871108), the Jilin Province-University Cooperative Construction Project–Special Funds for New Materials (No. SXGJSF2017-3), and the Jilin University Talents Cultivation Program for financial support.

Appendix A. Supplementary data

Supplementary material related to this article can be found, in the online version, at doi:https://doi.org/10.1016/j.cclet.2020.08.035.

References

[1] W.Q. Lim, G. Yang, S.Z.F. Phua, H. Chen, Y. Zhao, ACS Appl. Mater. Interfaces 11 (2019) 16391–16401.
[2] T. Sun, Y.S. Zhang, B. Pang, et al., Angew. Chem. Int. Ed. 53 (2014) 12320–12364.
[3] J. Zhou, G. Yu, F. Huang, Chem. Soc. Rev. 46 (2017) 7021–7053.
[4] M.W. Tibbitt, J.E. Dahlman, R. Langer, J. Am. Chem. Soc. 138 (2016) 704–717.
[5] M. Karimi, P. Sahandi Zangabad, S. Baghaee-Ravari, et al., J. Am. Chem. Soc. 139 (2017) 4584–4610.
[6] S.S. Said, S. Campbell, T. Hoare, Chem. Mater. 31 (2019) 4971–4989.
[7] M.X. Wu, Y.W. Yang, Adv. Mater. 29 (2017) 1606134.
[8] N. Zhao, L. Yan, X. Zhao, et al., Chem. Rev. 119 (2019) 1666–1762.
[9] Q. Hu, H. Li, L. Wang, H. Gu, C. Fan, Chem. Rev. 119 (2019) 6459–6506.
[10] J. Yang, Y.W. Yang, Small 16 (2020) 1906846.
[11] J.A. Barreto, W. O'Malley, M. Kubeil, et al., Adv. Mater. 23 (2011) H18–H40.
[12] J. Yang, Y.W. Yang, View 1 (2020) e20.
[13] X. Wang, M. Li, K. Ren, et al., Adv. Mater. 32 (2020) 2002160.
[14] K. Zhu, Y. Ju, J. Xu, et al., Acc. Chem. Res. 51 (2018) 404–413.
[15] G. Yang, S.Z.F. Phua, A.K. Bindra, Y. Zhao, Adv. Mater. 31 (2019) 1805730.
[16] F. Tang, L. Li, D. Chen, Adv. Mater. 24 (2012) 1504–1534.
[17] G. Yu, X. Zhao, J. Zhou, et al., J. Am. Chem. Soc. 140 (2018) 8005–8019.
[18] X. Li, H. Bai, Y. Yang, et al., Adv. Mater. 31 (2019) 1805092.
[19] S. Aryal, C.M.J. Hu, L. Zhang, ACS Nano 4 (2010) 251–258.
[20] S.Z.F. Phua, C. Xue, W.Q. Lim, et al., Chem. Mater. 31 (2019) 3349–3358.
[21] Z. Zheng, W.C. Geng, Z. Xu, D.S. Guo, Isr. J. Chem. 59 (2019) 913–927.
[22] M.J. Webber, R. Langer, Chem. Soc. Rev. 46 (2017) 6600–6620.
[23] T. Ogoshi, T. Kakuta, T.A. Yamagishi, Angew. Chem. Int. Ed. 58 (2019) 2197–2206.
[24] D. Xia, P. Wang, X. Ji, et al., Chem. Rev. 120 (2020) 6070–6123.
[25] N. Song, T. Kakuta, T.A. Yamagishi, Y.W. Yang, T. Ogoshi, Chem 4 (2018) 2029–2053.
[26] L. Liang, Y. Chen, X.M. Chen, Y. Zhang, Y. Liu, Chin. Chem. Lett. 29 (2018) 989–991.
[27] L.L. Tan, H. Li, Y. Tao, et al., Adv. Mater. 26 (2014) 7027–7031.
[28] L.L. Tan, Y. Zhu, Y. Jin, W. Zhang, Y.W. Yang, Supramol. Chem. 30 (2018) 648–654.
[29] D. Dai, Z. Li, J. Yang, et al., J. Am. Chem. Soc. 141 (2019) 4756–4763.
[30] M.X. Wu, Y.W. Yang, Polym. Chem. 10 (2019) 2980–2985.
[31] X. Wang, Z.J. Liu, E.H. Hill, et al., Matter 1 (2019) 848–861.
[32] X. Wang, J.R. Wu, F. Liang, Y.W. Yang, Org. Lett. 21 (2019) 5215–5218.
[33] H. Yao, Q. Zhou, Y. Zhang, et al., Chin. Chem. Lett. 31 (2020) 1231–1234.
[34] N. Song, X.Y. Lou, H. Yu, et al., Mater. Chem. Front. 4 (2020) 950–956.
[35] Z. Liu, J.R. Wu, C. Wang, et al., Chin. Chem. Lett. 30 (2019) 2299–2303.
[36] P. Li, Y. Chen, Y. Liu, Chin. Chem. Lett. 30 (2019) 1190–1197.
[37] H.B. Cheng, Y.M. Zhang, Y. Liu, J. Yoon, Chem 5 (2019) 553–574.
[38] X.Y. Lou, Y.P. Li, Y.W. Yang, Biotechnol. J. 14 (2018) 1800354.
[39] M.X. Wu, J. Gao, F. Wang, et al., Small 14 (2018) 1704440.
[40] Q.L. Li, Y. Sun, L. Ren, et al., ACS Appl. Mater. Interfaces 10 (2018) 29314–29324.
[41] J. Yang, D. Dai, X. Lou, et al., Theranostics 10 (2020) 615–629.
[42] Y. Chen, S. Sun, D. Lu, Y. Shi, Y. Yao, Chin. Chem. Lett. 30 (2019) 37–43.
[43] T. Ogoshi, S. Kanai, S. Fujinami, T.A. Yamagishi, Y. Nakamoto, J. Am. Chem. Soc. 130 (2008) 5022–5023.
[44] T. Ogoshi, T.A. Yamagishi, Y. Nakamoto, Chem. Rev. 116 (2016) 7937–8002.
[45] T. Ogoshi, N. Ueshima, F. Sakakibara, T.A. Yamagishi, T. Haino, Org. Lett. 16 (2014) 2896–2899.
[46] X.B. Hu, Z. Chen, L. Chen, et al., Chem. Commun. 48 (2012) 10999–11001.
[47] Y. Chen, H.Q. Tao, Y.H. Kou, et al., Chin. Chem. Lett. 23 (2012) 509–511.
[48] B. Li, Z. Meng, Q. Li, et al., Chem. Sci. 8 (2017) 4458–4464.
[49] N. Song, X.Y. Lou, L. Ma, H. Gao, Y.W. Yang, Theranostics 9 (2019) 3075–3093.
[50] X.Y. Lou, Y.W. Yang, Adv. Mater. 32 (2020) 2003263.
[51] Y. Cao, X.Y. Hu, Y. Li, et al., J. Am. Chem. Soc. 136 (2014) 10762–10769.
[52] X. Li, J. Han, X. Wang, et al., Mater. Chem. Front. 3 (2019) 103–110.
[53] K. Jie, M. Liu, Y. Zhou, et al., J. Am. Chem. Soc. 139 (2017) 2908–2911.
[54] J.R. Wu, Y.W. Yang, Chem. Commun. 55 (2019) 1533–1543.
[55] B. Gao, L.L. Tan, N. Song, K. Li, Y.W. Yang, Chem. Commun. 52 (2016) 5804–5807.
[56] J.R. Wu, C.Y. Wang, Y.C. Tao, et al., Eur. J. Org. Chem. 2018 (2018) 1321–1325.
[57] J.R. Wu, A.U. Mu, B. Li, et al., Angew. Chem. Int. Ed. 57 (2018) 9853–9858.
[58] D. Xia, Y. Li, K. Jie, B. Shi, Y. Yao, Org. Lett. 18 (2016) 2910–2913.

[59] T. Ogoshi, M. Hashizume, T.A. Yamagishi, Y. Nakamoto, Chem. Commun. 46 (2010) 3708–3710.
[60] G. Yu, M. Xue, Z. Zhang, et al., J. Am. Chem. Soc. 134 (2012) 13248–13251.
[61] W.H. Chen, W.C. Liao, Y.S. Sohn, et al., Adv. Funct. Mater. 28 (2018) 1705137.
[62] Z. He, X. Huang, C. Wang, et al., Angew. Chem. Int. Ed. 58 (2019) 8752–8756.
[63] Y. Wang, J. Yan, N. Wen, et al., Biomaterials 230 (2020) 119619.
[64] Y. Chen, Z. Huang, J.F. Xu, Z. Sun, X. Zhang, ACS Appl. Mater. Interfaces 8 (2016) 22780–22784.
[65] J. Chen, H. Ni, Z. Meng, et al., Nat. Commun. 10 (2019) 3546.
[66] C. Sun, H. Zhang, S. Li, et al., ACS Appl. Mater. Interfaces 10 (2018) 25090–25098.
[67] L. Yue, C. Sun, C.H.T. Kwong, R. Wang, J. Mater. Chem. B 8 (2020) 2749–2753.
[68] Y.F. Ding, J. Wei, S. Li, et al., ACS Appl. Mater. Interfaces 11 (2019) 28665–28670.
[69] L. Yue, C. Sun, Q. Cheng, et al., Chem. Commun. 55 (2019) 13506–13509.
[70] Q. Cheng, K.X. Teng, Y.F. Ding, et al., Chem. Commun. 55 (2019) 2340–2343.
[71] Q. Hao, Y. Chen, Z. Huang, et al., ACS Appl. Mater. Interfaces 10 (2018) 5365–5372.